





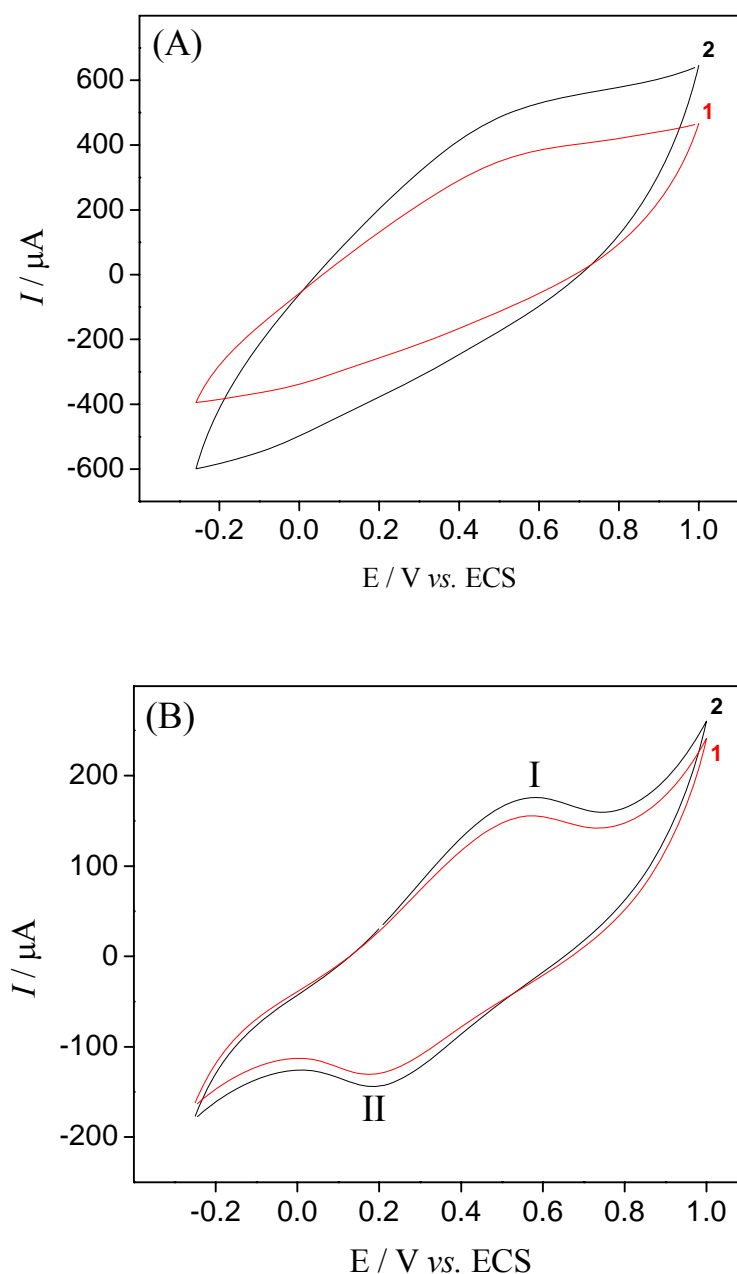




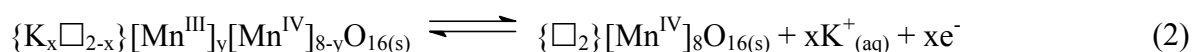
### 3.2. Electrochemical Behavior of the Sensor

The electrochemical and ion-sieve properties of the manganese oxides are frequently dependent on the synthetic process. The effect of the synthetic process on the electrochemical activity of the sensor based on hollandite-type manganese oxide was investigated by cyclic voltammetry. Figure 2 shows the cyclic voltammograms for samples synthesized by sol-gel and redox precipitation.

**Figure 2.** Cyclic voltammograms obtained at a scan of  $50 \text{ mV s}^{-1}$  for carbon paste modified with 20% (m/m) hollandite-type  $\text{MnO}_2$ : (1 – red curve) in TRIS buffer solution ( $\text{pH} = 8$ ); (2 – black curve) in TRIS buffer solution containing  $4.8 \times 10^{-4} \text{ mol L}^{-1}$  of potassium ions. Hollandite manganese oxide synthesized by (A) redox precipitation; (B) sol-gel route.



The carbon paste electrode modified with hollandite manganese oxide and synthesized by the sol-gel method showed a better electrochemical behaviour for potassium ions (see Figure 2B). This performance is related to the crystallinity degree and homogeneity of the oxide prepared. The particle shape and size of manganese oxide affect the way these particles are dispersed in carbon powder in sensor preparation. Larger particles favor a better dispersion where more of the manganese oxide is exposed and readily available for electrochemical activity. This surface may have more active redox sites as compared to that one of material synthesized by redox precipitation. The voltammetric profile of the sensor presented one anodic peak (peak I = +0.58 V vs. SCE) and another cathodic peak (peak II = +0.18 vs. SCE). This electrochemical activity is due to the extraction/insertion topotactic processes of the potassium ions from the hollandite structure [17]:



where { } denotes (2 × 2) tunnel sites, [ ] octahedral sites occupied by manganese, and □ vacant structural sites. The enhanced response to potassium ions occurs because the cathodic polarization of the sensor with hollandite-type manganese oxide is quite enough to reduce the manganese in the solid. Consequently, the potassium ions from the adjacent solution are able to diffuse through the hollandite structure to maintain the electroneutrality principle. In the absence of potassium ions (curve 1–Figure 2B), the voltammetric profile of the sensor shows a redox peak. Supposedly, that behavior can be related to vestiges of potassium ions in the hollandite-type manganese oxide that may have occurred during its preparation. The acid-treatment extracts 48% of K<sup>+</sup> ions from the metal ion inserted sample. This suggests that K<sup>+</sup> with a large ionic radius is tightly fixed on the (2 × 2) tunnel sites. In the presence of potassium ions (curve 2–Figure 2B), increase voltammetric response was observed for the sensor, confirming that the electrochemical response is a function of the insertion reaction of potassium ions in the hollandite structure.

The sensor composition was also investigated to check if the electrochemical response was limited by the electronic conductivity of the composite electrode. The amount of binder was kept constant while varying the amount of hollandite-type manganese oxide and graphite. The amount of manganese oxide in the carbon paste had a significant influence on the voltammetric response. The peak currents increase with amount of hollandite-type manganese oxide up to 20% (m/m). For amounts of manganese oxide higher than 25% (m/m) the anodic peak current decreased significantly. This occurs due to a decreasing of the graphite content in the paste and consequently the reduction of conductive area at the electrode surface. The best carbon-paste composition was found for an electrode composition of 20% (m/m) hollandite-type manganese oxide synthesized by sol-gel, 65% (m/m) graphite and 15% (m/m) mineral oil was used in further studies.

The variation of the peak currents and the potential peak separation ( $\Delta E_p = E_{pa} - E_{pc}$ ) of the sensor based on hollandite-type manganese oxide in solution containing  $4.8 \times 10^{-4}$  mol L<sup>-1</sup> potassium ions with scan rate (1–100 mV s<sup>-1</sup>) was studied. The  $\Delta E_p$  increase with variation of scan rate. These results allow to conclude that the charge transfer reaction of Mn<sup>(IV)</sup>/Mn<sup>(III)</sup> is controlled by diffusion of potassium ions in the solid phase. Hence, the solid-state diffusion of K<sup>+</sup> ions can be considered as the rate-determining step. The electrochemical insertion of potassium ions into the structure in the hollandite-type manganese oxide consists of three processes that are: solution mass transport, dehydration and transfer at the solid surface, and solid-state diffusion [18].

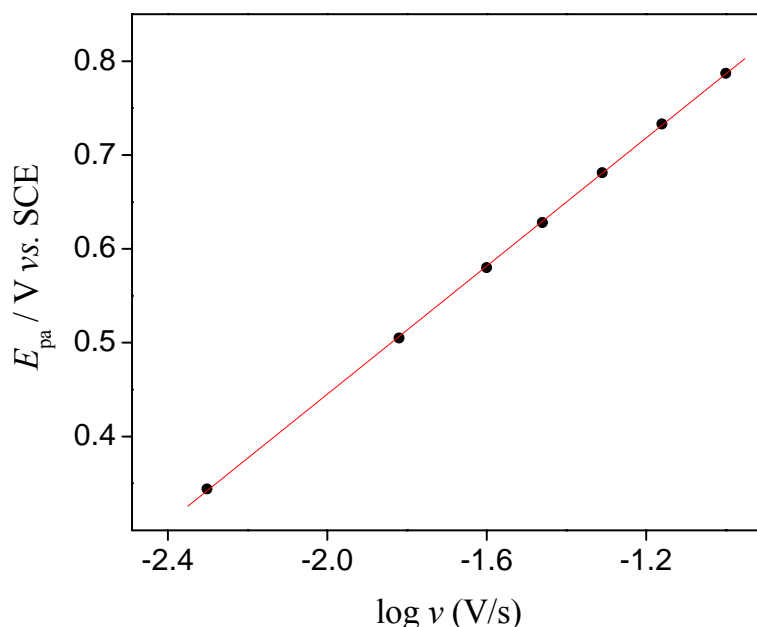
Linear relations were obtained when plotting the peak currents versus the square root of the scan rate revealing a diffusion controlled rate reaction. The following linear relationships were obtained:

$$I_{pa} (\mu\text{A}) = -26.7 + 34.8 v^{1/2} (\text{mV}^{1/2} \text{s}^{-1/2}) \quad r = 0.9991 \quad (3)$$

$$I_{pc} (\mu\text{A}) = 51.1 + 33.5 v^{1/2} (\text{mV}^{1/2} \text{s}^{-1/2}) \quad r = 0.9999 \quad (4)$$

The apparent electrochemical rate constant  $k_e$  and the electron-transfer coefficient  $\alpha_{\text{anodic}}$  were calculated for the sensor according to the method described by Larivon [20,21]. It has been shown by Laviron that for a surface redox couple,  $\alpha_{\text{anodic}}$  and  $k_e$  can be determined from the variation of  $E_{\text{pa}}$  with scan rate. Figure 3 presents the plot of  $E_{\text{pa}}$  (V) versus  $\log v$  ( $\text{V s}^{-1}$ ) of the sensor in Tris buffer solution (pH = 8) containing  $4.8 \times 10^{-4} \text{ mol L}^{-1}$  potassium ions.

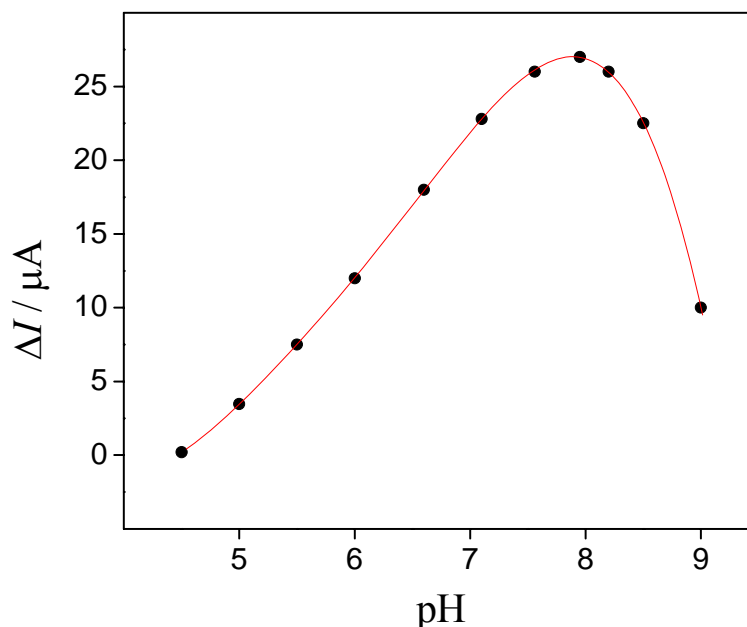
**Figure 3.** Dependence of  $E_{\text{pa}}$  with  $\log(v)$  for the sensor in Tris buffer solution (pH = 8) containing  $4.8 \times 10^{-4} \text{ mol L}^{-1}$  potassium ions.



The  $E_{\text{p}}-\log v$  plots gave one straight line with slopes of  $2.303RT/(1-\alpha_{\text{anodic}})nF$  for the anodic branch, where  $R$  is the gas constant,  $T$  the absolute temperature,  $F$  the Faraday constant and  $n$  number of electrons involved in the redox couple. Considering that the number of electrons involved in the redox process is 1, the calculated value for the coefficient  $\alpha_{\text{anodic}}$  was 0.83. These results suggest the redox process tends towards an irreversible system. The apparent electrochemical rate constant can then be determined by applying the equation  $k_e = 2.303\alpha_{\text{anodic}}nFv_0/RT$ , in which the value of scan rate ( $v_0$ ) is determined by extrapolation of the linear branch at higher scan rates and its intersection with the constant peak potential, represented by the peak of the voltammogram at the lower scan rate. The observed value was  $k_e = 0.4 \text{ s}^{-1}$ .

The influence of the pH on the electrochemical response of the sensor was studied over a pH range between 4.5–9 controlled with TRIS buffer in the absence and in the presence of potassium ions of  $4.8 \times 10^{-4} \text{ mol L}^{-1}$ . The cyclic voltammograms of the sensor based on hollandite-type  $\text{MnO}_2$  were performed at scan rate of  $50 \text{ mV s}^{-1}$  in different pHs.

**Figure 4.** pH dependence of the voltammetric response of the sensor in a TRIS buffer solution of different pHs in presence of  $4.8 \times 10^{-4}$  mol L<sup>-1</sup> potassium ions. Scan rate = 50 mV s<sup>-1</sup>. The anodic peak current ( $\Delta I_{pa}/\mu\text{A}$ ) was obtained by the difference of the currents in the presence and absence of potassium ions.



The obtained result indicated that the current value of anodic peak is strongly influenced by the pH and reached a maximum value at pH 8 (see Figure 4). According to Feng *et al.* [17], extraction of potassium ions in structure and surface disproportionation reaction of the manganese oxide ( $2\text{Mn}^{3+}_{(s)} \rightarrow \text{Mn}^{4+}_{(s)} + \text{Mn}^{2+}_{(aq)}$ ) in the presence of cation ions occur at acid pH. With this disproportionation reaction, the amount of manganese oxide in the electrode surface also decreases, leading to smaller peak currents. For pH 8.5 the value of peak current decreased considerably due to another surface formation of non-electroactive manganese oxide. Recently, Teixeira *et al.* [12,13] obtained similar behavior when studied the voltammetric properties of a carbon-paste electrode modified with spinel-type manganese oxide.

The dependence of anodic peak current of the sensor with the pre-concentration was also investigated. The voltammetric responses of the sensor were realized in a solution containing  $4.8 \times 10^{-4}$  mol L<sup>-1</sup> of potassium ions after pre-concentration at  $-0.25$  V vs. SCE for different times. The difference of the anodic peak currents in the presence and absence of potassium ions increases with the increasing of the pre-concentration time between 0 and 100 s. It has become nearly constant due to the surface saturation of the oxide with potassium ion. Based on this experiment, it is demonstrated the ability of the hollandite to accommodate non-electroactive cation and promote the electroactivity in function of the insertion potassium is the manganese oxide.

### 3.3. Analytical Performance of the Sensor

The influence of alkaline ( $\text{Na}^+$ ,  $\text{K}^+$ ,  $\text{Rb}^+$  and  $\text{Cs}^+$ ) and earth alkaline ( $\text{Mg}^{2+}$ ,  $\text{Ca}^{2+}$ ,  $\text{Sr}^{2+}$ ,  $\text{Ba}^{2+}$ ) ions on the response of the sensor has been studied. For this study, the current values of the sensor were

obtained by injection of sample volumes containing alkaline and alkaline-earth ions in the absence and presence of potassium ions. Table 1 shows the relative current (%) calculated by the difference of the currents in the presence and absence of the cation in study.

A characteristic feature is that the selectivity sequences relate to the pore size of the manganese oxide. The selectivity sequences are  $\text{Cs}^+ < \text{Rb}^+ < \text{Na}^+ \leq \text{Li}^+ < \text{NH}_4^+ < \text{K}^+$  and  $\text{Mg}^{2+} < \text{Ca}^{2+} < \text{Sr}^{2+} < \text{Ba}^{2+} < \text{K}^+$  for sensor based on hollandite-type manganese oxide. The hollandite-type  $\text{MnO}_2$  ion-sieves show a large adsorptive for potassium ion at low pH range [18,22]. However, at high pH range, the adsorptive capacity increases with a decrease of ionic radius, except for alkaline-earth ions. This suggests that the insertion reaction is subject to the steric interaction between the cation ions in the tunnel and it becomes predominant. When electrochemical measurements were recorded in solution containing potassium ions, it was not observed a significant increase in the relative current indicating that the insertion reaction occurs preferably with potassium ions. This behavior is related to cavity size of the  $\text{MnO}_2$ , dehydration energy and especially to ionic mobility of the metallic ion in aqueous solution. Potassium ions are expected to be more mobile than lithium, sodium, all alkaline-earth ions, and might therefore enhance the rate of charge transfers, evidenced by decreasing the influence of these cations in the relative currents.

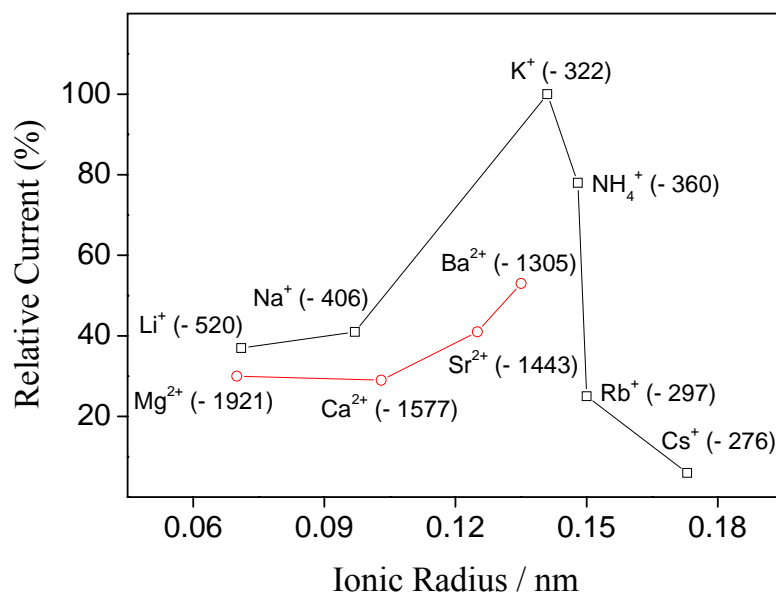
**Table 1.** Interference dependence of the voltammetric responses of the sensor based on hollandite-type manganese oxide in TRIS buffer solution (pH = 8) containing  $4.8 \times 10^{-4} \text{ mol L}^{-1}$  of alkaline and alkaline-earth metal ions in the absence and presence of potassium ions ( $4.7 \times 10^{-4} \text{ mol L}^{-1}$ ).

metallic cation	Absence of $\text{K}^+$ ions	Presence of $\text{K}^+$ ions
	$I_{\text{relative}}$ (%)	$I_{\text{relative}}$ (%)
$\text{K}^+$	100	100
$\text{Li}^+$	67	37
$\text{Na}^+$	64	41
$\text{Rb}^+$	53	25
$\text{Cs}^+$	36	6
$\text{Mg}^{2+}$	35	30
$\text{Ca}^{2+}$	43	29
$\text{Sr}^{2+}$	50	41
$\text{Ba}^{2+}$	71	53
$\text{NH}_4^+$	86	78

The relative currents of the sensor observed upon addition of alkali and alkaline earth metal ions into a  $4.8 \times 10^{-4} \text{ mol L}^{-1}$  potassium ion background electrolyte solution were plotted as a function of ionic radius of the cations in Figure 5 (with respective enthalpies of dehydration). As it is seen, there are obviously size selectivities to the ions with an ionic radius around 0.141 nm. Ammonium ion caused a serious interference on the electrochemical response of the sensor. As the ionic radius of ammonium ion (0.148 nm) is close to that of potassium ion (0.141 nm),  $\text{NH}_4^+$  can be inserted into the tunnel structure of hollandite. The weaker responses to divalent cations compared to monovalent ions having similar ionic radius may be due to their higher energies of dehydration which is needed for uptake of cations into the solid phase from the aqueous solution. Hydration of an ion depends on the

electrostatic attraction of water molecules to that ion. Because attraction of water molecules around an ion depends on that ion's density of charge, smaller ions (and thus ions of greater ionic potential) attract more water molecules. The result is the inverse relationship between non-hydrated radius and hydrated radius. The relatively small amount of  $\text{Li}^+$  and  $\text{Na}^+$  loading suggests that lithium and sodium ions are inserted into the tunnel in a partially hydrated form.

**Figure 5.** Plot of relative current of the sensor *versus* ionic radius of alkaline and alkaline-earth ions. The values in parentheses represent the dehydration energy (23) for each cation study.



The optimal potential of the working electrode had to be found to achieve the most sensitive determination of the potassium ion. Thus, we studied the dependence of current responses on potential in the range from 0.4 to 0.9 V *vs.* SCE in the absence and presence of the potassium ion under continuous stirring at 300 rpm. The resulting hydrodynamic voltammograms are shown in Figure 6. The height of current responses of the potassium increased with increasing potential. However, the background signal (absence of the potassium ions) was too high with the increase of applied potential. An operating potential of +0.80 V *vs.* SCE was selected for all further studies due to the good reproducibility and stability of the sensor.

In order to obtain an analytical curve for the developed sensor, chronoamperometric studies for potassium determination were carried out at different concentrations in  $0.1 \text{ mol L}^{-1}$  TRIS (pH 8.0) under continuous stirring at 300 rpm. The measurements were realized with applied at potential of  $-0.25 \text{ V vs. SCE}$  by 30 s and then was at potential level of 0.80 V. The useful net current signals recorded at 60 seconds.

**Figure 6.** Influence of the applied potential on the anodic current of the sensor. (1) background current. (2) peak height of the current response.

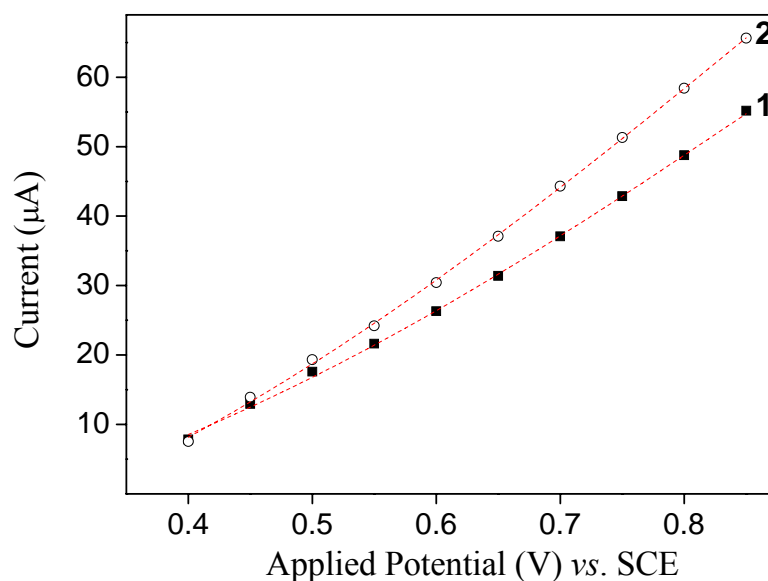
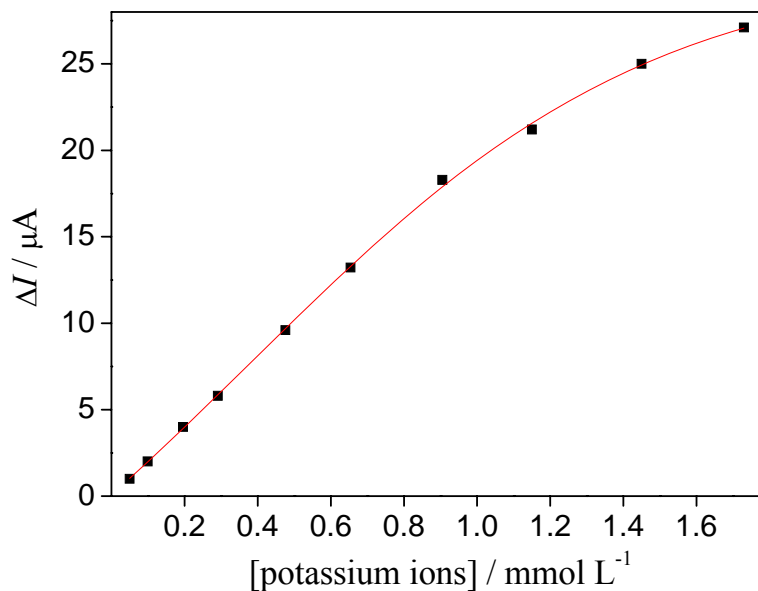


**Figure 7.** Calibration curve for potassium ion using sensor based on hollandite-type manganese oxide. Potential step:  $-0.25$  V to  $0.80$  V vs. SCE. Stirring rate: 300 rpm



The proposed sensor showed a linear response range from  $4.97 \times 10^{-5}$  up to  $9.05 \times 10^{-4}$  mol L<sup>-1</sup> (Figure 7), which can be expressed according to the following equation  $\Delta I$  ( $\mu\text{A}$ ) =  $0.007 + 20.2$  [ $\text{K}^+$ ] ( $\text{mmol L}^{-1}$ ) with a correlation coefficient of 0.9997 ( $n = 7$ ). At higher concentrations ( $> 9.05 \times 10^{-4}$  mol L<sup>-1</sup>), deviation from linearity occurs. The detection limit calculated according to the recommendations of IUPAC [24] were  $1.61 \times 10^{-6}$  mol L<sup>-1</sup> of potassium ions, presenting good sensitivity of this sensor for potassium dosage.

#### 4. Conclusions

Hollandite-type manganese oxide shows strong promise for potential application as an amperometric sensor for potassium ions. The mechanism of the sensor depends on the electrochemical activity of the manganese oxide with extraction/insertion topotactic processes of the potassium ions from the hollandite structure. With an operating potential of +0.80 V *versus* SCE, the current signals are linearly proportional to potassium ion concentration in the range  $4.97 \times 10^{-5}$  to  $9.05 \times 10^{-4}$  mol L<sup>-1</sup> with a correlation coefficient of 0.9997. During successive cycles (100 cycles) in supporting electrolyte, the peak currents decreased by less 7%. The lifetime of the sensor was approximately seven months.

#### Acknowledgements

The scholarship granted by CNPq (no. 372010/2006-7) to A.S.L. and research support are gratefully acknowledged. The authors acknowledge Prof. P. M. Seraphim (FCT-UNESP-Brazil) for the English revision. The authors thank SJT.

#### References

1. Malavolti, E.; Cagnini, A.; Caputo, G.; Della, L.C.; Mascini, M. An optimized optrode for continuous potassium monitoring in whole blood. *Anal. Chim. Acta.* **1999**, *401*, 129-136.
2. Harrison T.R.; Adams, R.D.; Bennett, I.L.; Resnik, W.H.; Thorn, G.W.; Wintrobe M.M. *Principles of Internal Medicine*, 5th ed.; McGraw-Hill, New York, USA, 1966.
3. A.O.A.C. *Official Methods of Analysis of the Association of Official Analytical Chemists*, 15<sup>th</sup> ed.; Helrich, K. (Ed.); A.O.A.C.: Gaithersburg, MD, USA, 1990; pp. 503-504.
4. Doku, G.N.; Gadzekpo, V.P.Y. Simultaneous determination of lithium, sodium and potassium in blood serum by flame photometric flow-injection analysis. *Talanta* **1996**, *43*, 735-739.
5. Ng, R.H.; Sparks, K.M.; Statland, B.E. Colorimetric determination of potassium in plasma and serum by reflectance photometry with a dry-chemistry reagent. *Clin. Chem* **1992**, *38*, 1371-1372.
6. Gallardo, J.; Alegret, S.; Muñoz, R.; De Román, M.; Leija, L.; Hernández, P.R.; Del Valle, M.; An electronic tongue using potentiometric all-solid-state PVC-membrane sensors for the simultaneous quantification of ammonium and potassium ions in water. *Anal. Bioanal. Chem.* **2003**, *377*, 248-256.
7. Garcia, C.A.B.; Júnior L.R.; Neto G.O. Determination of potassium ions in pharmaceutical samples by FIA using a potentiometric electrode based on ionophore nonactin occluded in EVA membrane. *J. Pharm. Biomed. Anal.* **2003**, *31*, 11-18.
8. Karyakin, A.A. Prussian blue and its analogues: electrochemistry and analytical applications. *Electroanalysis* **2001**, *13*, 813-819.
9. Brock, S.L.; Duan, N.; Tian, Z.R.; Giraldo, O.; Zhou, H.; Suib, S. A review of porous manganese oxide materials. *Chem. Mater.* **1998**, *10*, 2619-2628.
10. Ferracin, L.C.; Amaral, F.A.; Bocchi, N. Characterization and electrochemical performance of the spinel LiMn<sub>2</sub>O<sub>4</sub> prepared from ε-MnO<sub>2</sub>. *Solid State Ionics* **2000**, *130*, 215-219.

11. Teixeira, M.F.S.; Cavalheiro, E.T.G.; Bergamini, M.F.; Moraes F.C.; Bocchi, N. Use of a carbon paste electrode modified with spinel-type manganese oxide as a potentiometric sensor for lithium ions in flow injection analysis. *Electroanalysis* **2004**, *16*, 633-639.
12. Teixeira, M.F.S.; Bergamini, M.F.; Bocchi, N. Lithium ions determination by selective pre-concentration and differential pulse anodic stripping voltammetry using a carbon paste electrode modified with a spinel-type manganese oxide. *Talanta* **2004**, *62*, 603-609.
13. Teixeira, M.F.S.; Moraes, F.C.; Fatibello-Filho, O.; Bocchi, N. Voltammetric determination of lithium ions in pharmaceutical formulation using a  $\lambda$ -MnO<sub>2</sub>-modified carbon-paste electrode. *Anal. Chim. Acta.* **2001**, *443*, 249-255.
14. Teixeira, M.F.S.; Moraes, F.C.; Fatibello-Filho, O.; Ferracin, L.C.; Rocha-Filho, R.; Bocchi, N. A novel  $\lambda$ -MnO<sub>2</sub>-based graphite-epoxy electrode for potentiometric determination of acids and bases. *Sens. Actuators B* **1999**, *56*, 169-174.
15. Teixeira, M.F.S.; Lima, A.S.; Seraphim, P.M.; Bocchi, N. Development of an amperometric sensor for potassium ions. In *Proceeding of the First International Conference on Biomedical Electronics and Devices*, Funchal, Portugal, **2008**, *1*, 198-201.
16. Suib, S.L. Porous manganese oxide octahedral molecular sieves and octahedral layered materials. *Acc. Chem. Res.* **2008**, *41*, 479-487.
17. Feng, Q.; Kanoh, H.; Miyai, Y.; Ooi, K. Alkali metal ions insertion/extraction reactions with hollandite-type manganese oxide in the aqueous phase. *Chem. Mater.* **1995**, *7*, 148-153.
18. Feng, Q.; Kanoh, H.; Ooi, K. Manganese oxide porous crystals. *J. Mater. Chem.* **1999**, *9*, 319-333.
19. Guinier, A. *Theorie et Pratique de la Radiocristallographie*; Guinier, A., Ed.; Dunod: Paris, France, 1964.
20. Laviron, E. General expression of the linear potential sweep voltammogram in the case of diffusionless electrochemical systems. *J. Electroanal. Chem.* **1979**, *101*, 19-28.
21. Laviron, E.; Roullier, L. General expression of the linear potential sweep voltammogram for a surface redox reaction with interactions between the adsorbed molecules. Applications to modified electrodes. *J. Electroanal. Chem.* **1980**, *115*, 65-74.
22. Tani, Y.; Umezawa, Y. Alkali metal ion-selective electrodes based on relevant alkali metal ion doped manganese oxides. *Mikrochim. Acta* **1998**, *129*, 81-90.
23. Smith, D.W. Ionic hydration enthalpies. *J. Chem. Educ.* **1977**, *54*, 540-542.
24. *Analyst*. Analytical Methods Committee: London, UK, 1987; pp. 199-204.
25. Ching, S.; Roark, J.L.; Duan, N.; Suib, S.L. Sol-gel route to the tunneled manganese oxide cryptomelane *Chem. Mater.* **1997**, *9*, 750-754.
26. DeGuzman, R.N.; Shen, Y.F.; Neth, E.J.; Suib, S.L.; O'Young, C.L.; Levine, S.; Newsam, J.M. Synthesis and characterization of octahedral molecular sieves (OMS-2) having the hollandite structure. *Chem. Mater.* **1994**, *6*, 815-821.